

## Supplementary Information

### Impacts of ionic liquid capping on morphology and photocatalytic performance of SbPO<sub>4</sub> crystals

Shunqiang Chen,<sup>a</sup> Yutong Di,<sup>a</sup> Taohai Li<sup>\*a</sup>, Feng Li<sup>a</sup> and Wei Cao<sup>b</sup>

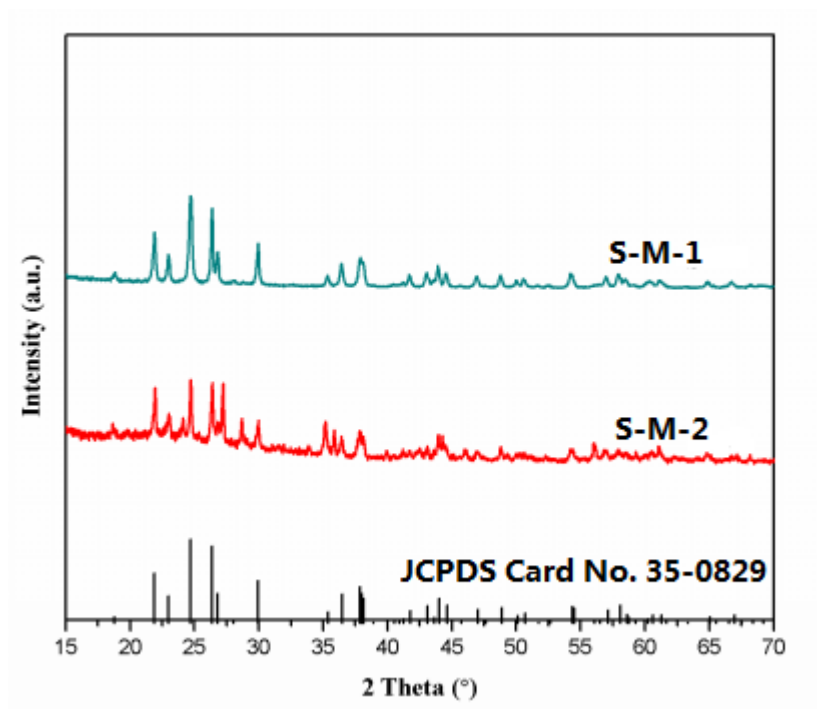


Figure S1. XRD patterns of SbPO<sub>4</sub> samples prepared by hydrothermal method with different Sb/P mole ratios.

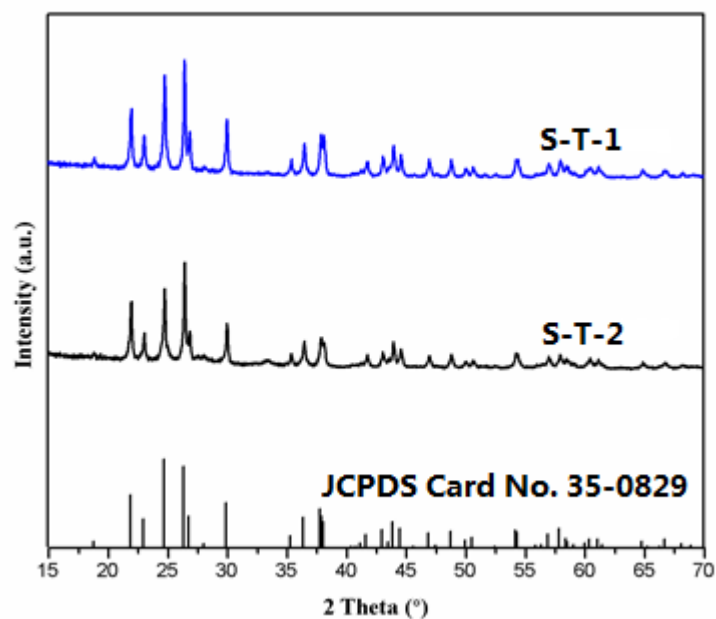


Figure S2. XRD patterns of  $\text{SbPO}_4$  samples obtained at different hydrothermal time.

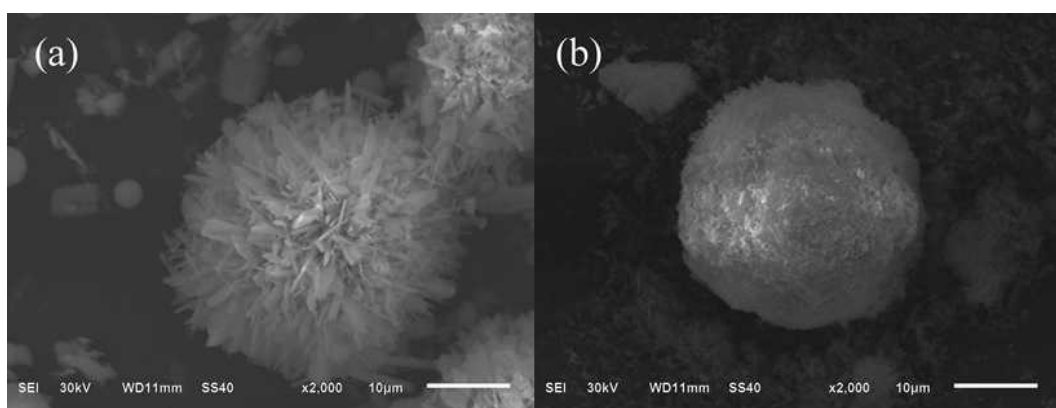


Figure S3. SEM images of the  $\text{SbPO}_4$  synthesized with different Sb/P mole ratios: (a) S-M-1, (b) S-M-2.

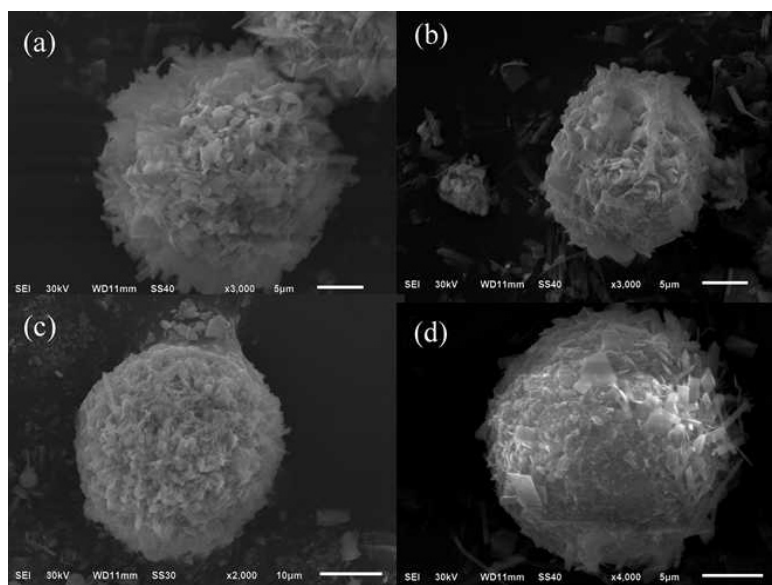


Figure S4. SEM images of the  $\text{SbPO}_4$  synthesized with different reaction time: (a,b) S-T-1, (c) S-P-2, (d) S-T-2.

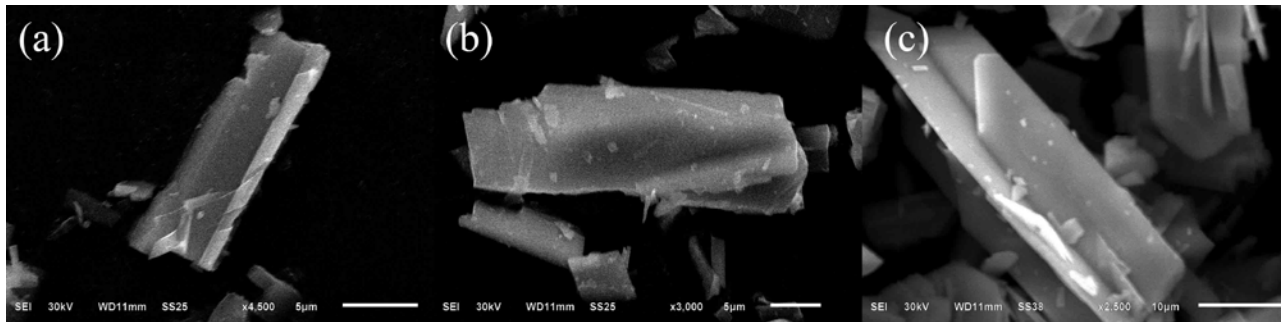


Figure S5. SEM images of the synthesized  $\text{SbPO}_4$ : (a) S-O-1, (b) S-O-2, (c) S-O-3.

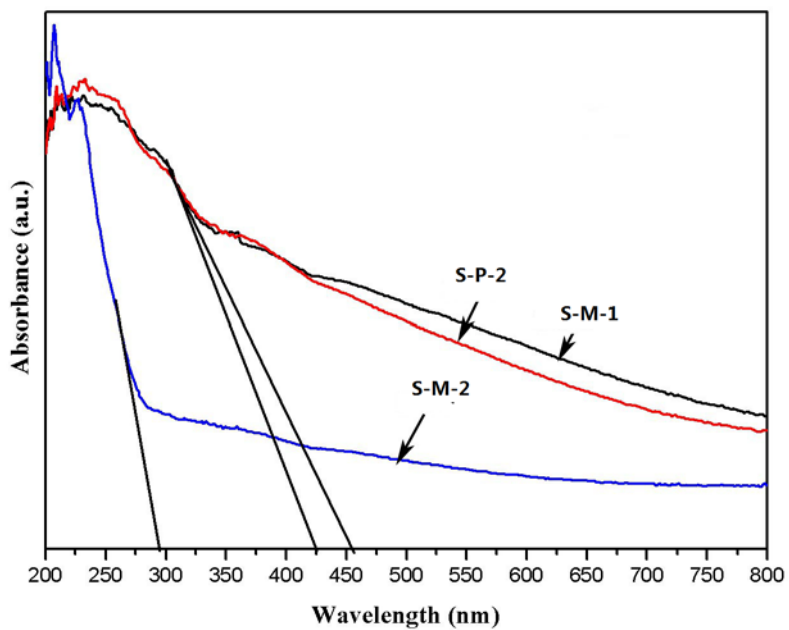


Figure S6. UV-Vis diffuse reflection spectra of  $\text{SbPO}_4$  at different Sb/P mole ratios and S-P-2.

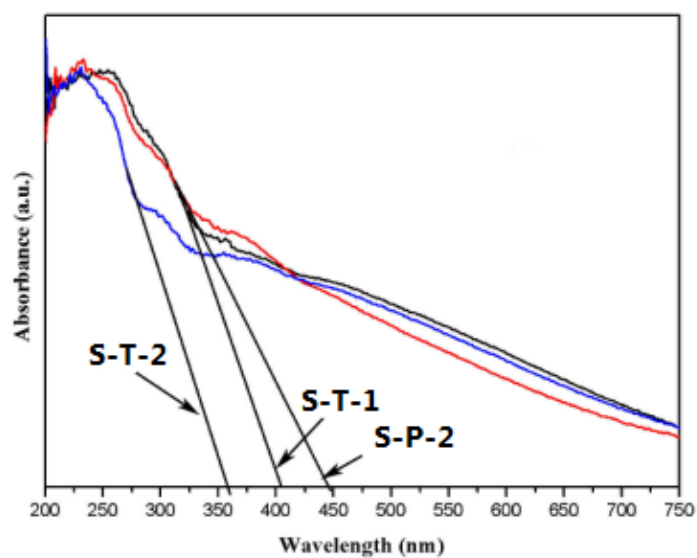


Figure S7. UV-Vis diffuse reflection spectra of  $\text{SbPO}_4$  at different reaction time and S-P-2.

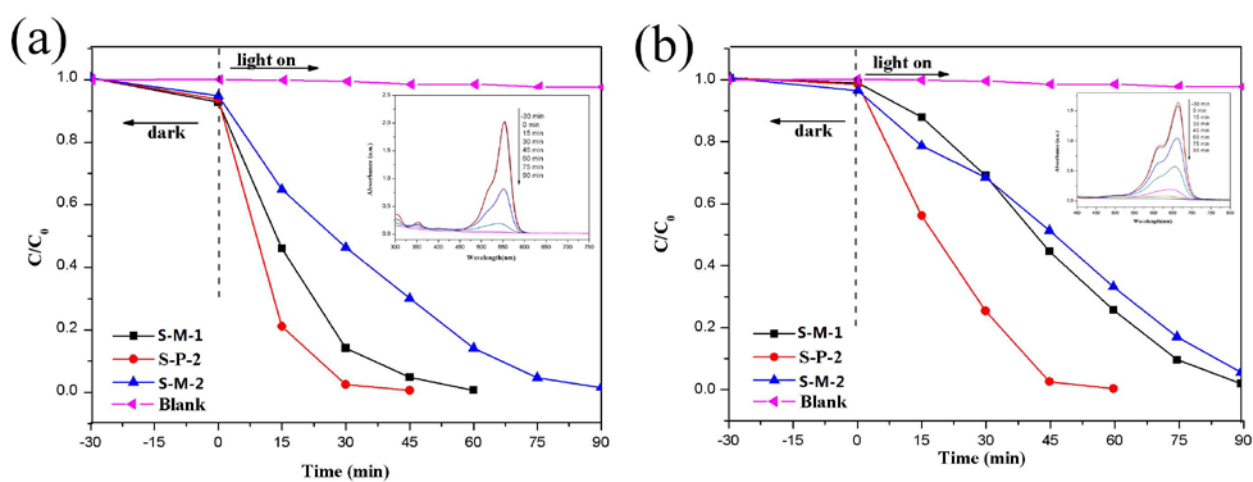


Figure S8. The degradation efficiency of S-M-1, S-P-2, S-M-2, (a) RhB, (b) MB

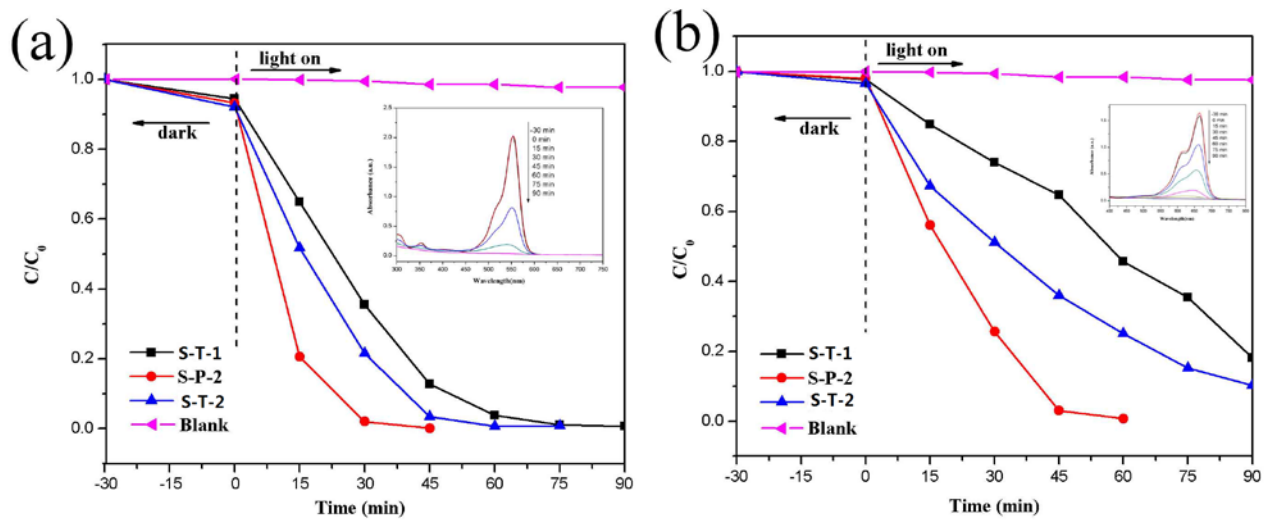


Figure S9. The degradation efficiency of S-T-1, S-P-2, S-T-2, (a) RhB, (b) MB

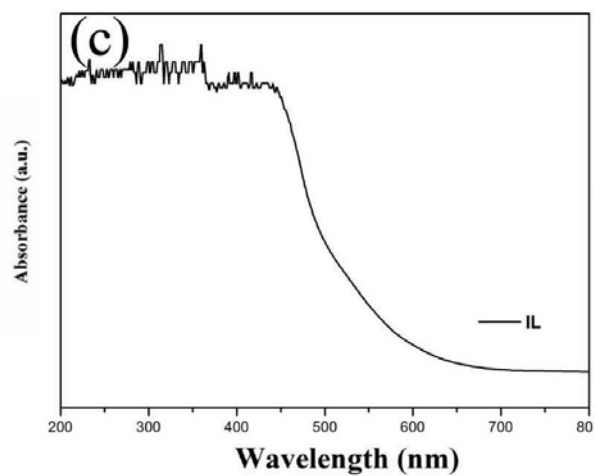


Figure S10. UV-Vis diffuse reflection spectra of pure ILs.

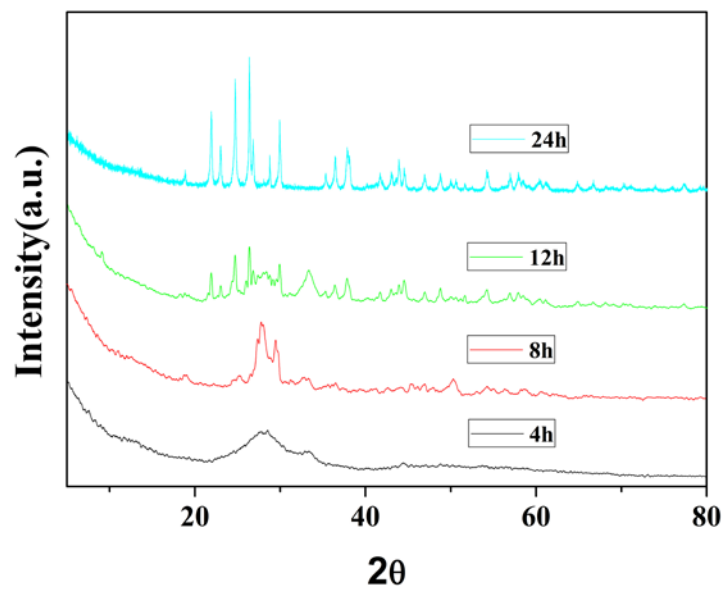


Figure S11. XRD of the SbPO<sub>4</sub> fabricated at different reaction time: 4, 8, 12, 24.

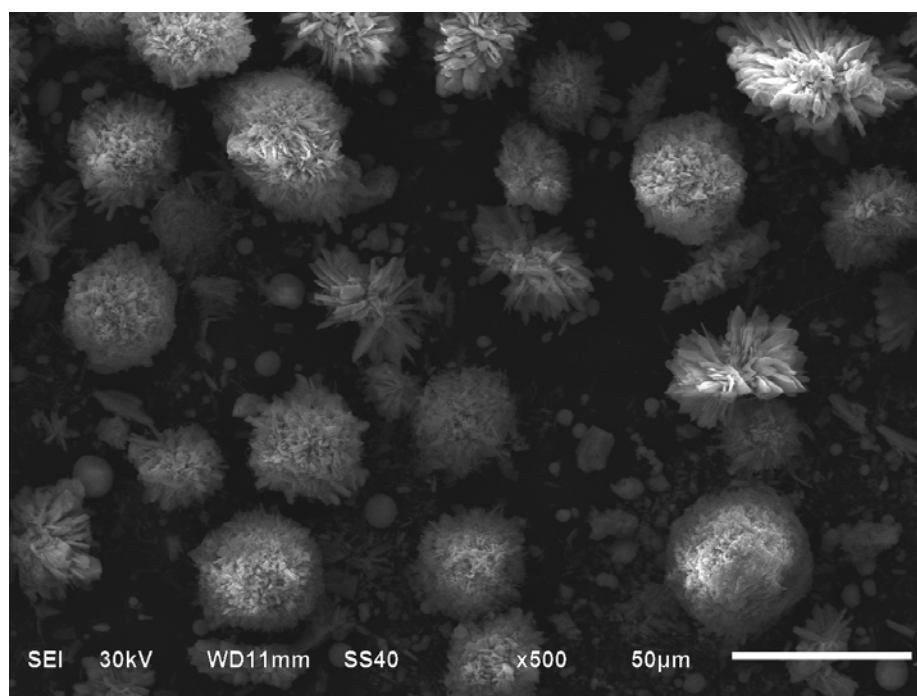


Figure S12. The low SEM of S-P-2.

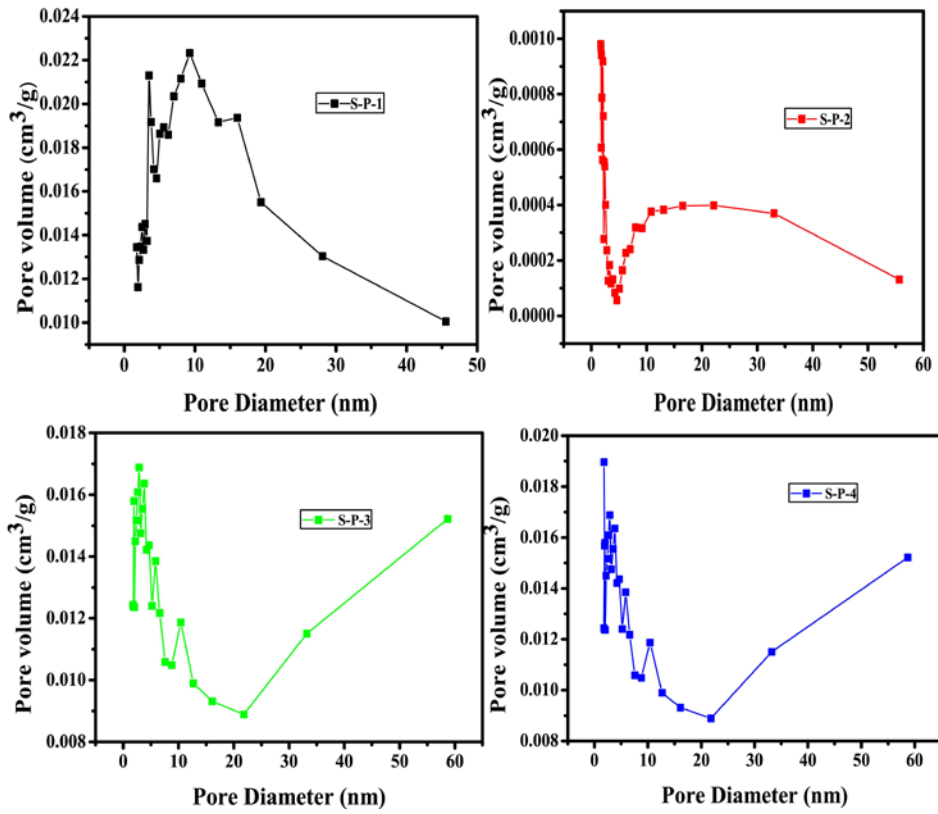


Figure S13. The pore diameter distributions images of samples